

Vector-Meson-Dominance Predictions on Inelastic Electron-Proton Scattering*

C. F. CHO, G. J. GOUNARIS,† AND J. J. SAKURAI

The Enrico Fermi Institute and the Department of Physics, The University of Chicago, Chicago, Illinois 60637

(Received 9 June 1969)

We present predictions of the (recently proposed) vector-meson-dominance model for inelastic electron-proton scattering in a manner that can be compared directly with forthcoming experimental data. For large scattering angles ($\theta=18^\circ-34^\circ$), a spectacular variation is predicted in $d^2\sigma/d\Omega dE'$ as a function of the missing mass or q^2 , in sharp contrast with the published 6° data, which exhibit a very weak q^2 dependence. We also give our νW_2 and $(q^2/\nu)W_1$ as functions of ν/q^2 .

RECENTLY one of us¹ proposed a model of high-energy inelastic electron-proton scattering based on vector-meson dominance. In this paper we point out some of the more striking features of the model in such a manner that a direct comparison can be made with forthcoming experimental data.

The model of Ref. 1 predicts that, in the diffraction (or "continuum") region, the Hand cross sections σ_T and σ_S measurable in inelastic electron-proton scattering are given (in the notation of Ref. 1) by

$$\begin{aligned}\sigma_T(q^2, \nu) &= [m_V^2/(q^2 + m_V^2)]^2 \sigma_{\gamma p}(K), \\ \sigma_S(q^2, \nu) &= [m_V^2/(q^2 + m_V^2)]^2 \\ &\quad \times (q^2/m_V^2)(K/\nu)^2 \xi(K) \sigma_{\gamma p}(K) \quad (1) \\ &\quad [K = \nu - q^2/2m_p = (s - m_p^2)/2m_p],\end{aligned}$$

where the parameter ξ characterizes the ratio of the total ρp cross sections with different helicities:

$$\xi(K) = \sigma_{\rho p}^{(\lambda=0)}/\sigma_{\rho p}^{(\lambda=\pm 1)}.$$

In Ref. 1 the vector-meson mass m_V is set to the ρ -meson mass, but in this paper we treat it as a variable parameter to simulate possible contributions from higher-mass states.

The cross sections appearing in Eq. (1) are related to the double-differential cross section for inelastic electron-proton scattering in the laboratory system as follows:

$$\begin{aligned}d^2\sigma/d\Omega dE' &= \Gamma_T(\sigma_T + \epsilon\sigma_S), \\ \Gamma_T &= \frac{\alpha K E'}{2\pi^2 q^2 E 1 - \epsilon}, \quad (2) \\ \epsilon &= 1/[1 + 2(1 + \nu^2/q^2) \tan^2(\frac{1}{2}\theta)].\end{aligned}$$

Equation (2) can also be written in terms of the Drell-

Walecka form factors W_1 and W_2 :

$$\begin{aligned}\frac{d^2\sigma}{d\Omega dE'} &= \frac{\alpha^2 \cos^2(\frac{1}{2}\theta)}{4E^2 \sin^4(\frac{1}{2}\theta)} \\ &\quad \times [W_2(q^2, \nu) + 2 \tan^2(\frac{1}{2}\theta) W_1(q^2, \nu)], \quad (3)\end{aligned}$$

with

$$\begin{aligned}W_1 &= (K/4\pi^2\alpha)\sigma_T, \\ W_2 &= (K/4\pi^2\alpha)[q^2/(q^2 + \nu^2)](\sigma_T + \sigma_S).\end{aligned} \quad (4)$$

The quantity that is directly measured in the SLAC-MIT experiment² (still in progress) is $d^2\sigma/d\Omega dE'$, with the incident energy E and the scattered electron angle θ fixed; as the final electron energy E' ($=E-\nu$) is varied, q^2 and the missing (hadronic) mass \sqrt{s} also vary:

$$\begin{aligned}q^2 &= 2EE'(1 - \cos\theta), \\ s &= 2m_p(E - E') + m_p^2 - q^2.\end{aligned} \quad (5)$$

In Figs. 1(a)-1(d) we present our theoretical predictions on $d^2\sigma/d\Omega dE'$ as a function of \sqrt{s} and also of q^2 for typical values of E and θ at which measurements have been (or are being) made.³ The total hadronic cross section $\sigma_{\gamma p}(K)$ is assumed to take a constant value of 125 μb throughout, even though recent direct measurements appear to suggest a slow decrease in $\sigma_{\gamma p}(K)$ between $K=3$ and 15 GeV. Three different assumptions are made on m_V and ξ :

- (i) $\xi=1, m_V=m_\rho,$
- (ii) $\xi=2, m_V=m_\rho,$
- (iii) $\xi=1, m_V=m_\phi.$

All the assumptions are compatible with the 6° data (the only published data) within accuracies of about 30%, provided the missing mass is in the continuum region; an example of this is shown in Fig. 1(a) for $E=13.5$ GeV.

As already emphasized by the experimentalists of Ref. 2, the most striking feature of the 6° data is the absence of a strong q^2 dependence in the continuum

* Supported in part by the U. S. Atomic Energy Commission.
† Present address: Physics Department, Brookhaven National Laboratory, Upton, N. Y. 11973.

¹ J. J. Sakurai, Phys. Rev. Letters **22**, 981 (1969). Vector-meson-dominance models for inelastic electron-proton scattering have also been considered by S. Berman and W. Schmidt (unpublished) and by G. A. Piketty and L. Stodolsky, in Proceedings of the Topical Conference on Weak Interactions, CERN Geneva, 1969, p. 75 [CERN Report No. 69-7 (unpublished)].

² The status of the SLAC-MIT experiment as of the summer of 1968 is summarized in W. K. H. Panofsky, in *Proceedings of the Fourteenth International Conference on High-Energy Physics, Vienna, 1968* (CERN, Geneva, 1968), pp. 36-37. See also L. W. Mo and Y. S. Tsai, Rev. Mod. Phys. **41**, 205 (1969).

³ We have actually calculated our predictions for every angle and energy at which measurements have been (or are being) made. They are available upon request.

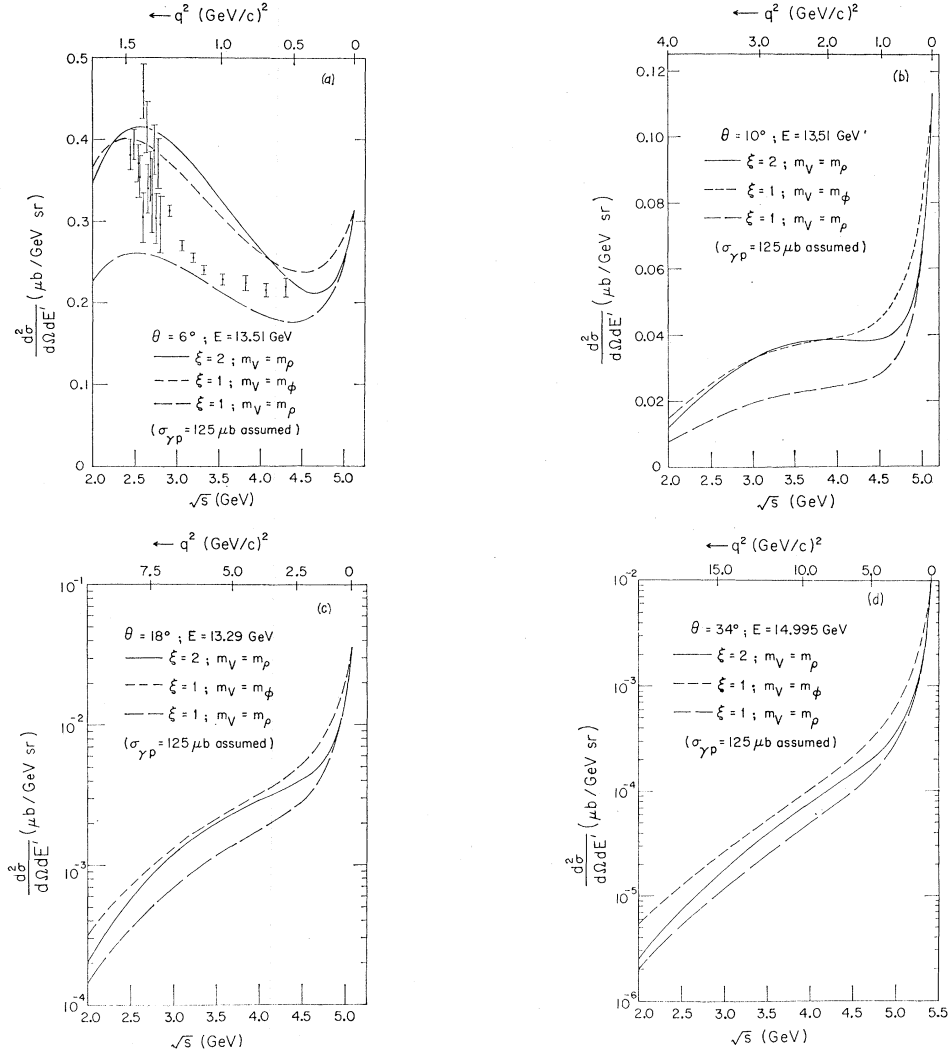


FIG. 1. Predictions on the double-differential cross section (with $\sigma_{\gamma p} = 125 \mu\text{b}$): (a) $\theta = 6.0^\circ$, $E = 13.51 \text{ GeV}$; (b) $\theta = 10.0^\circ$, $E = 13.51 \text{ GeV}$; (c) $\theta = 18.0^\circ$, $E = 13.29 \text{ GeV}$; (d) $\theta = 34.0^\circ$, $E = 15.00 \text{ GeV}$.

region. We predict that this feature still persists in the 10° data as long as q^2 is restricted to be greater than 1 $(\text{GeV}/c)^2$, as seen, for instance, from Fig. 1(b). However, for the larger-angle data (18° , 26° , and 34°) a completely different picture is predicted to emerge. The double differential cross section $d^2\sigma/d\Omega dE'$ [or, equivalently, the unseparated inelastic form factor $W_2 + 2 \times \tan^2(\frac{1}{2}\theta)W_1$] varies so rapidly with the missing mass or q^2 that we must plot it on a logarithmic scale. As an example, we may look at our predictions for $\theta = 34^\circ$, $E = 15 \text{ GeV}$ [Fig. 1(d)]; the double-differential cross section is predicted to drop by three orders of magnitude between $q^2 = 0$, $\sqrt{s} = 5.4 \text{ GeV}$ and $q^2 = 16 \text{ (GeV}/c)^2$, $\sqrt{s} = 2.5 \text{ GeV}$.

One of the most important predictions of our model is the large ratio of the longitudinal to the transverse cross section implied by Eq. (1):

$$\sigma_S(q^2, \nu) / \sigma_T(q^2, \nu) = (q^2 / m_V^2) \xi(K) (1 - q^2 / 2m_p \nu)^2. \quad (6)$$

As is well known, σ_S and σ_T can be separated by making a generalized Rosenbluth plot, in which we plot against ϵ the quantity $\sigma_T + \epsilon \sigma_S$ measured at different angles but at fixed values of q^2 and ν . We present in Fig. 2 our theoretical predictions on $\sigma_T + \epsilon \sigma_S$ at $q^2 = 4 \text{ (GeV}/c)^2$ and $\sqrt{s} = 3 \text{ GeV}$. As is clear from Fig. 2, cross sections measured to accuracies of about 15% should be able to discriminate various assumptions we may make on ξ and m_V .

The dimensionless quantity νW_2 has been an object of intense theoretical speculations in recent months. In our model it is given by

$$\nu W_2 = (m_V^2 / 4\pi^2 \alpha) (K / \nu) \frac{1}{1 + (q^2 / \nu^2)} \left(\frac{1}{1 + (m_V^2 / q^2)} \right)^2 \times [\xi(K) (K / \nu)^2 + m_V^2 / q^2] \sigma_{\gamma p}(K). \quad (7)$$

This expression is plotted as a function of ν/q^2 in Figs. 3(a)–3(c).⁴ Even though our model possesses a non-trivial Bjorken limit (i.e., $\nu W_2 \neq 0$ as $q^2 \rightarrow \infty$, ν/q^2 finite), the manner in which νW_2 approaches this asymptotic limit is rather slow.⁵ In passing, we may remind the reader that from an experimental point of view νW_2 is, in general, not a directly accessible quantity; to obtain W_2 in a model-independent way, it is essential to separate σ_S and σ_T , which can be done well only in a limited region of the q^2 - ν plane.

For completeness we also present our W_1 , where it is profitable to work with the dimensionless quantity $(q^2/\nu)W_1$:

$$(q^2/\nu)W_1(q^2, \nu) = (m_V^2 \sigma_{\gamma p} / 4\pi^2 \alpha) (1 - q^2/2m_V \nu) \times (1 + q^2/m_V^2)^{-1} (1 + m_V^2/q^2)^{-1}. \quad (8)$$

This function is plotted in Fig. 4. At fixed q^2 , $(q^2/\nu)W_1$ (as well as νW_2) approaches a constant for large values of ν/q^2 , in agreement with Pommeranchukon exchange.⁶ In the limit $q^2 \rightarrow \infty$ with ν/q^2 fixed, $(q^2/\nu)W_1$ (or W_1 itself) goes to zero; in other words, our $(q^2/\nu)W_1$ has a trivial Bjorken limit, which is characteristic of the

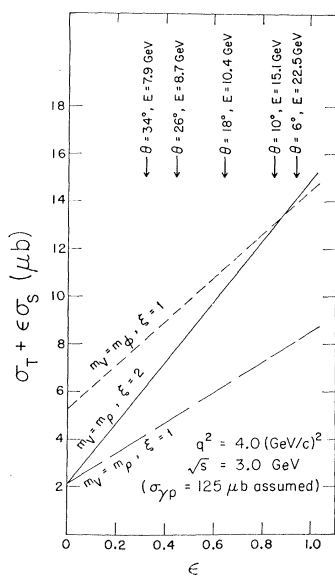


FIG. 2. Generalized Rosenbluth plot at $q^2=4.0$ (GeV/c)², $\sqrt{s}=3.0$ GeV ($K=4.33$ GeV, $\nu=6.46$ GeV).

⁴ The quantity actually plotted is νW_2 multiplied by $(100 \mu\text{b})/\sigma_{\gamma p}(K)$, so, to obtain νW_2 , multiply the ordinate by 1.25 if $\sigma_{\gamma p}(K)$ turns out to be $125 \mu\text{b}$.

⁵ We therefore feel that it is dangerous to infer the asymptotic form of νW_2 from Fig. 23 of Panofsky's rapporteur talk (Ref. 2).

⁶ H. D. I. Abarbanel, M. L. Goldberger, and S. B. Treiman, Phys. Rev. Letters 22, 500 (1969); H. Harari, *ibid.* 22, 1079 (1969).

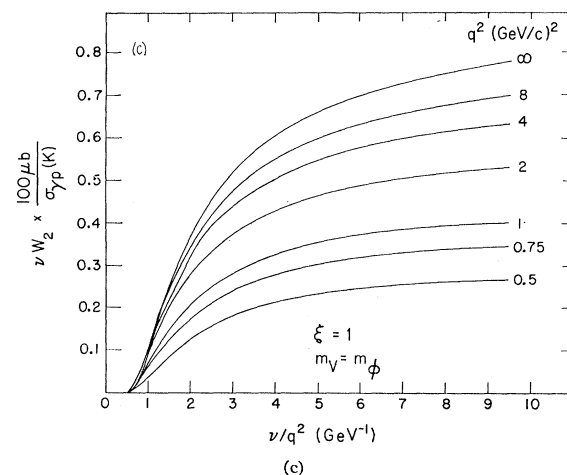
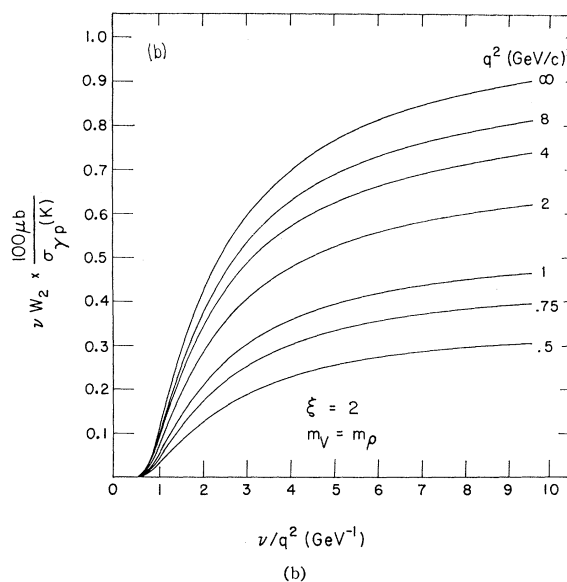
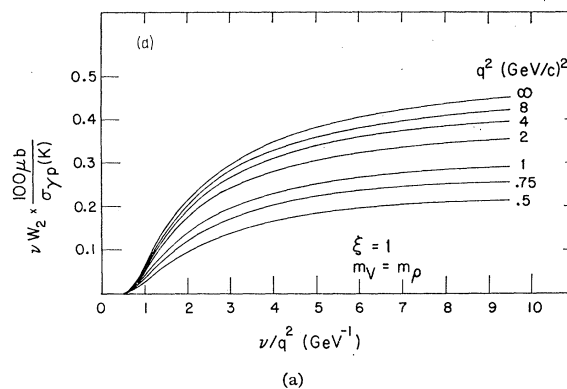


FIG. 3. Predictions on νW_2 : (a) $m_V = m_\rho$, $\xi = 1$; (b) $m_V = m_\rho$, $\xi = 2$; (c) $m_V = m_\phi$, $\xi = 1$.

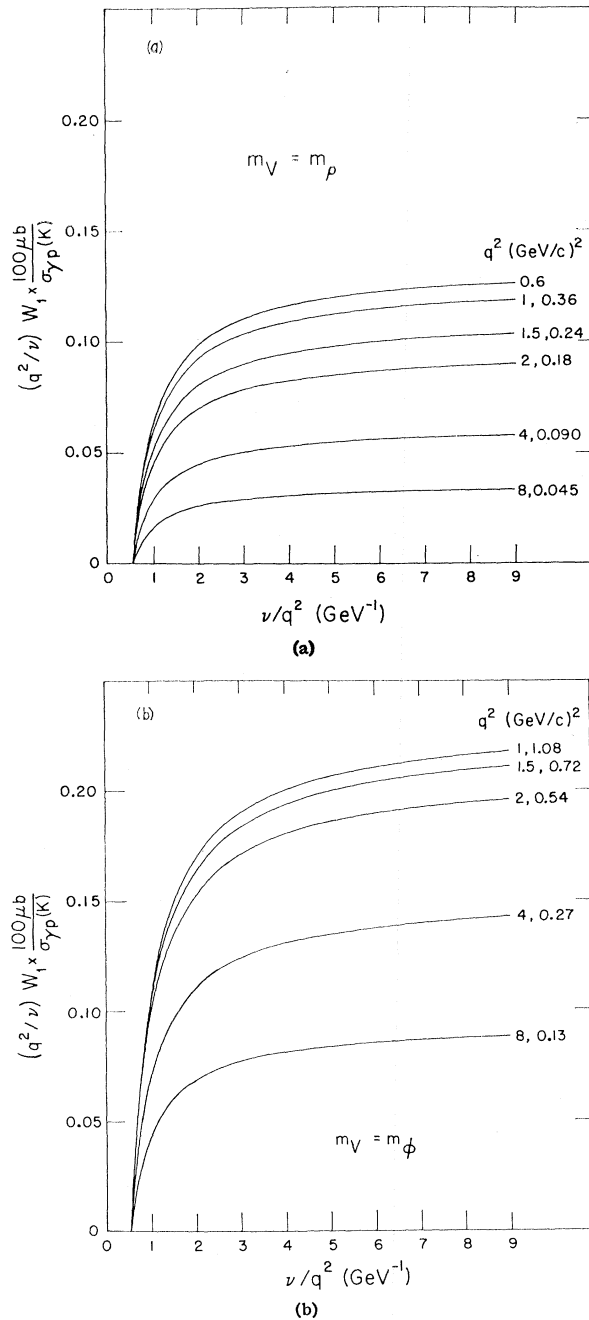


FIG. 4. Predictions on $(q^2/\nu)W_1$: (a) $m_V = m_\rho$; (b) $m_V = m_\phi$.

high-energy behavior based on the gauge-field algebra.⁷ Notice, however, that our νW_1 does possess a nontrivial Bjorken limit:

$$\lim_{q^2 \rightarrow \infty, \nu/q^2 \text{ finite}} \nu W_1 = (m_V^4 \sigma_{\gamma p} / 4\pi^2 \alpha) (\nu/q^2)^2 (1 - q^2/2m_p \nu). \quad (9)$$

We would like to suggest that, upon completion of the experiment, the data be fitted to our theoretical predictions using three different prescriptions:

- (i) Set $m_V = m_\rho$ and let ξ be a variable parameter.
- (ii) Set $\xi = 1$ and let m_V be a variable parameter.
- (iii) Let both m_V and ξ be variable parameters.

It may, of course, turn out that the effective mass of the vector meson seen in inelastic electron-proton scattering is q^2 -dependent, e.g., $m_V^2 \approx m_\rho^2$ at $q^2 = 1 (\text{GeV}/c)^2$ and $m_V^2 \approx 2m_\rho^2$ at $q^2 = 10 (\text{GeV}/c)^2$. After all, we are applying vector-meson dominance up to absurdly high values of q^2 (viz., $q^2 \approx 30m_\rho^2$).

Note added in proof. The 6° and 10° data of the SLAC-MIT group are now published; E. D. Bloom *et al.*, Phys. Rev. Letters **23**, 930 (1969); M. Breidenbach *et al.*, *ibid.* **23**, 935 (1969). A detailed comparison with our model will be presented elsewhere. More recently preliminary results on σ_S - σ_T separation based on the larger angle data have been reported: See, e.g., R. E. Taylor, in Proceedings of the 1969 International Symposium on Electron and Photon Interactions at High-Energies, University of Liverpool, 1969 (unpublished). At $q^2 = 4 (\text{GeV}/c)^2$ and $\sqrt{s} = 2, 3, 4 \text{ GeV}$, it appears that $\sigma_S/\sigma_T \lesssim 0.5$, in disagreement with our predictions. It is possible that our model based on diffraction scattering works better when $s \gg q^2$.

It is a pleasure to thank Dr. L. W. Mo for informing us of the energies and angles at which experimental data are being taken.

⁷ C. G. Callan, Jr., and D. J. Gross, Phys. Rev. Letters **22**, 156 (1969).